© 2019. Published by The Company of Biologists Ltd | Journal of Cell Science (2019) 132, jcs228486. doi:10.1242/jcs.228486

RESEARCH ARTICLE

Differential requirements for the EF-hand domains of human centrin 2 in primary ciliogenesis and nucleotide excision repair

Ebtissal M. Khouj[1], Suzanna L. Prosser[1,2], Haruto Tada[3,4], Weng Man Chong[5], Jung-Chi Liao[5], Kaoru Sugasawa[3,4] and Ciaran G. Morrison[1,*]

ABSTRACT

Centrin 2 is a small conserved calcium-binding protein that localizes to the centriolar distal lumen in human cells. It is required for efficient primary ciliogenesis and nucleotide excision repair (NER). Centrin 2 forms part of the xeroderma pigmentosum group C protein complex. To explore how centrin 2 contributes to these distinct processes, we mutated the four calcium-binding EF-hand domains of human centrin 2. Centrin 2 in which all four EF-hands had been mutated to ablate calcium binding (4DA mutant) was capable of supporting *in vitro* NER and was as effective as the wild-type protein in rescuing the UV sensitivity of centrin 2-null cells. However, we found that mutation of any of the EF-hand domains impaired primary ciliogenesis in human TERT-RPE1 cells to the same extent as deletion of centrin 2. Phenotypic analysis of the 4DA mutant revealed defects in centrosome localization, centriole satellite assembly, ciliary assembly and function and in interactions with POC5 and SFI1. These observations indicate that centrin 2 requires calcium-binding capacity for its primary ciliogenesis functions, but not for NER, and suggest that these functions require centrin 2 to be capable of forming complexes with partner proteins.

This article has an associated First Person interview with the first author of the paper.

KEY WORDS: Primary cilium, Centrosome, Centriole, Centrin 2, CETN2, Nucleotide excision repair

INTRODUCTION

Primary cilia are membrane-bounded, antenna-like structures that arise from the surface of most human cell types to sense and transduce chemical and mechanical signals (Goetz and Anderson, 2010). Defective primary cilium formation or activity causes a complex range of human developmental disorders that affect the kidney, eye, liver, brain and skeleton, collectively termed the ciliopathies (Braun and Hildebrandt, 2017). Furthermore, loss of primary ciliation is commonly seen in cancer and has been suggested as an early step in oncogenesis (Sánchez and Dynlacht, 2016).

The 'stalk' of the cilium, the axoneme, consists of nine doublet microtubules extending from one end of the basal body, a centriole that docks to the plasma membrane during ciliogenesis (Sorokin, 1962). Centrioles show a striking polarity because of their microtubule-based structure. The minus ends of the centriolar microtubule triplets define the proximal ends of the centrioles. At the distal ends, two sets of radially arranged appendages distinguish the older, 'mother' centriole. Distal appendages (DAs), the structures forming 'transition fibers' in basal bodies, are necessary for the mother centriole to act as the basal body during ciliogenesis (Tanos et al., 2013). Reverse genetic experiments have established a core set of DA proteins that constitutively localize to these structures and are required for ciliogenesis (Graser et al., 2007; Tanos et al., 2013). Recent super-resolution imaging of the pinwheel-like blades that comprise the DAs has positioned this core set extending outward from the mother centriole in the following order: CEP83–CEP89–SCLT–CEP164, with FBF1 located between the blades (Yang et al., 2018).

Another crucial requirement for axoneme outgrowth is the removal of CP110 (also known as CCP110) and its partner protein CEP97 from the mother centriole distal end (Spektor et al., 2007; Tsang et al., 2008). CP110 interacts with components of the centriolar distal lumen, including centrin 2, and is involved in centriole duplication and elongation, acting as a length-regulatory centriole cap (Chen et al., 2002; Tsang et al., 2006; Kleylein-Sohn et al., 2007). Centrosomal-P4.1-associated protein (CPAP, also known as CENPJ) is a tubulin-binding regulator of centriole length (Tang et al., 2009). Overexpression of CPAP increases centriole length, whereas its depletion impedes centriole duplication and elongation (Tang et al., 2009). CP110 has the reciprocal effect of CPAP in centriole length regulation: its depletion causes centriole lengthening and its overexpression blocks centriole extension (Chen et al., 2002; Spektor et al., 2007). Current models suggest that CP110 blocks ciliogenesis by impeding the interaction of CEP290 with Rab8, a small GTPase required for vesicle docking and ciliogenesis. Another CP110 interactor, Talpid3 (also known as KIAA0586), also contributes to the appropriate regulation of Rab8 during maturation of the ciliary vesicle (Kobayashi et al., 2014). However, knockout experiments in mouse indicate a requirement for CP110 in subdistal appendage assembly and ciliary vesicle docking (DAs were not examined in this experiment), suggesting that the roles of CP110 change during ciliogenesis (Yadav et al., 2016). One mechanism that removes CP110 during ciliogenesis involves the CEP164-dependent activation of tau tubulin B kinase (TTBK2) at basal bodies, although the relevant TTBK2 targets have not yet been defined (Cajanek and Nigg, 2014; Goetz et al., 2012). Another mechanism controlling CP110 removal involves its ubiquitination and subsequent degradation through the $SCF^{cyclin\ F}$ ubiquitin ligase complex (D'Angiolella et al., 2010). This activity is opposed by the de-ubiquitinating enzyme USP33 (Li et al., 2013). The precise details of the activities and regulation of CP110 at specific stages during ciliogenesis remain to be defined.

Centrin 2 (CETN2, also known as caltractin) is a member of a family of small calmodulin-like proteins that bind calcium through four

[1]Centre for Chromosome Biology, School of Natural Sciences, National University of Ireland Galway, Galway H91 W2TY, Ireland. [2]Lunenfeld-Tanenbaum Research Institute, Sinai Health System, 600 University Avenue, Toronto, Ontario M5G 1X5, Canada. [3]Biosignal Research Center, 1-1 Rokkodai-cho, Nada-ku, Kobe, Hyogo 657-8501, Japan. [4]Graduate School of Science, Kobe University, 1-1 Rokkodai-cho, Nada-ku, Kobe, Hyogo 657-8501, Japan. [5]IAMS Academia Sinica, No 1 Roosevelt Rd Sec 4, 10617 Taipei City, Taiwan.

*Author for correspondence (Ciaran.Morrison@nuigalway.ie)

S.L.P., 0000-0001-6373-9716; C.G.M., 0000-0003-2401-7029

Received 3 December 2018; Accepted 29 August 2019

Journal of Cell Science (2019) 132, jcs228486. doi:10.1242/jcs.228486

EF-hand domains. They are found in the distal centriolar lumen and in several other locations throughout the cell (Paoletti et al., 1996; Dantas et al., 2012). Centrins are required for centriole formation in lower eukaryotes (Zhang and He, 2011) but, despite some siRNA studies indicating a role in centriole formation in mammalian cells, our data using gene knockouts in chicken and human cells have shown that centriole duplication is normal in the absence of centrin 2 (Dantas et al., 2011; Prosser and Morrison, 2015; Salisbury et al., 2002). Centrin 2 is a component of the xeroderma pigmentosum group C (XPC) complex and ensures efficient nucleotide excision repair (NER) of various helix-distorting DNA lesions (Araki et al., 2001; Nishi et al., 2005; Acu et al., 2010; Dantas et al., 2011; Daly et al., 2016). Interestingly, it is required for normal ciliogenesis in mice and human cells (Graser et al., 2007; Mikule et al., 2007; Prosser and Morrison, 2015; Ying et al., 2014), with its deficiency causing abnormal regulation of the distal end of the mother centriole. How centrin 2 contributes to the two processes of NER and primary ciliogenesis is not clear.

In this study, we used a mutagenesis approach to dissect the functions of the EF-hand domains of human centrin 2. We found a marked distinction between the requirements for centrin 2 calcium-binding capacity in NER and primary ciliogenesis. The pronounced requirement for centrin and its EF-hands in primary ciliogenesis suggests that a key role for centrin 2 lies in allowing multimeric protein assembly through calcium-dependent conformational shifts.

RESULTS

Analysis of the EF-hand domains of centrin 2 in centriolar localization and DNA damage responses

To explore the functions of the four EF-hand domains of human centrin, we used site-directed mutagenesis to ablate their calcium-binding capacity. We mutated to alanine the first aspartic acid residue of the loop region of the EF-hands, which is necessary for Ca^{2+} binding (Geiser et al., 1991; Gifford et al., 2007; Vonderfecht et al., 2011), at D41, D77, D114 and D150. We then generated mutants of the N-terminal and C-terminal pairs of EF-hands, and a mutant in which all four EF-hands were mutated (4DA). Myc-tagged versions of these mutants, with the exception of the D150A single mutant, and the wild-type centrin 2 protein were stably expressed in *CETN2* knockout human TERT-RPE1 cells (Prosser and Morrison, 2015); we selected clones with expression levels similar to those of the endogenous protein (Fig. 1A). We then tested for the ability of these mutants to localize to centrioles. As shown in Fig. 1B,C, single EF-hand mutations were compatible with centriolar localization, but the mutation of the two C-terminal or all four EF-hands abrogated centrin 2 localization to centrioles.

Notably, despite the impact on centriole localization, a clonogenic survival assay showed that the centrin 2 4DA mutant was as capable as wild-type centrin 2 at rescuing defective NER in centrin 2 null cells (Daly et al., 2016) (Fig. 2A). Furthermore, an *in vitro* assay indicated that the centrin 2 4DA mutant was fully capable of stimulating the early stages of NER of 6-4 photoproducts (Fig. 2B,C). We next tested whether loss of the EF-hands impacted on the interaction between centrin 2 and XPC. As shown in Fig. 2D, recombinant 4DA centrin 2 was capable of binding to XPC–RAD23B, although somewhat less efficiently than the wild-type protein. Together, these data show that the roles of centrin 2 in NER are independent of the EF-hands.

We next tested whether the centriolar satellites (Tollenaere et al., 2015) were affected by mutation of the EF-hands of centrin 2. Notably, mutation of any of the EF-hands caused a decline in

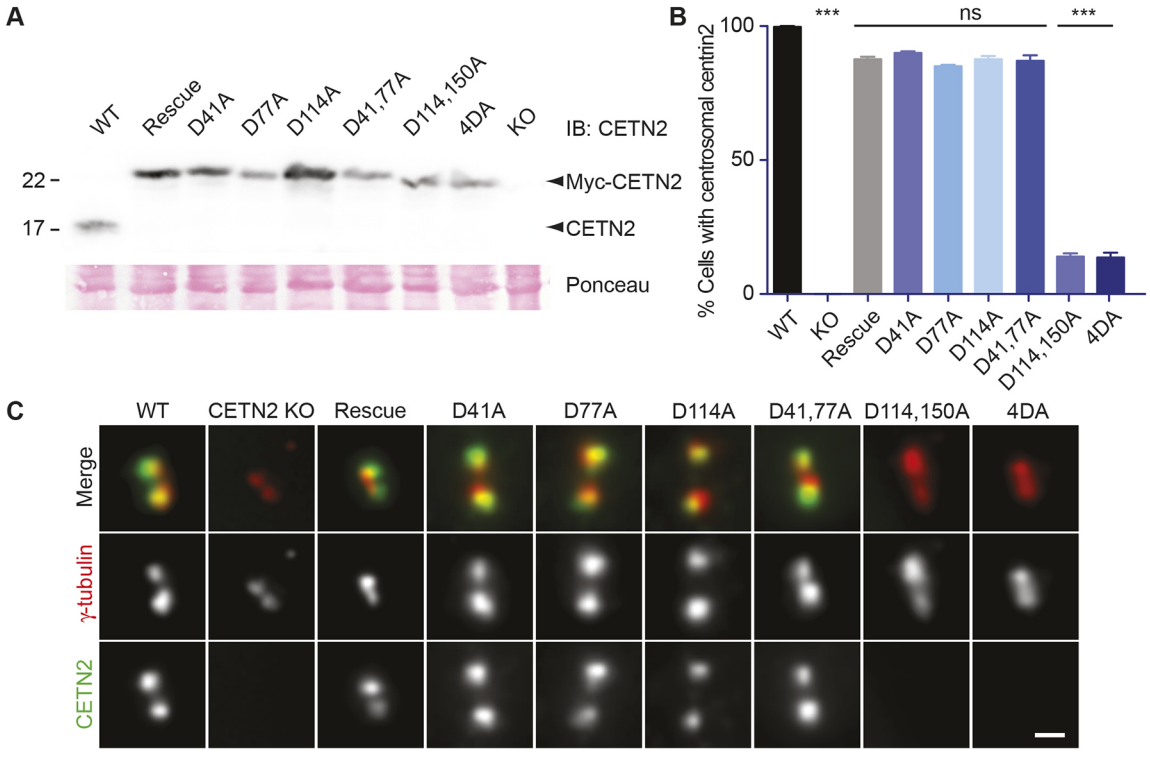

Fig. 1. Centrin 2 EF-hand mutants are deficient in centrosome localization. (A) Immunoblot showing the protein expression levels of endogenous centrin 2 and the myc–centrin 2 transgenes in the clones used here. Ponceau staining of the membrane was used as a loading control. WT, wild-type hTERT-RPE1 cells; KO, *CETN2* knockout; Rescue, *CETN2*$^{-/-}$ cells that express the wild-type form of centrin 2. Size markers (in kDa) are indicated on the left. (B) Percentage (mean±s.e.m.) of cells with centrosomal centrin 2, as determined by co-staining for γ-tubulin, scored from three separate experiments in which at least 100 cells were counted. ns, not significant; ***P<0.001 compared with controls by one-way ANOVA and Dunnett's multiple comparison test. (C) Immunofluorescence micrograph showing the localization of centrin 2 relative to γ-tubulin in wild-type cells and the indicated centrin 2 mutants. Scale bar: 1 µm.

Journal of Cell Science (2019) 132, jcs228486. doi:10.1242/jcs.228486

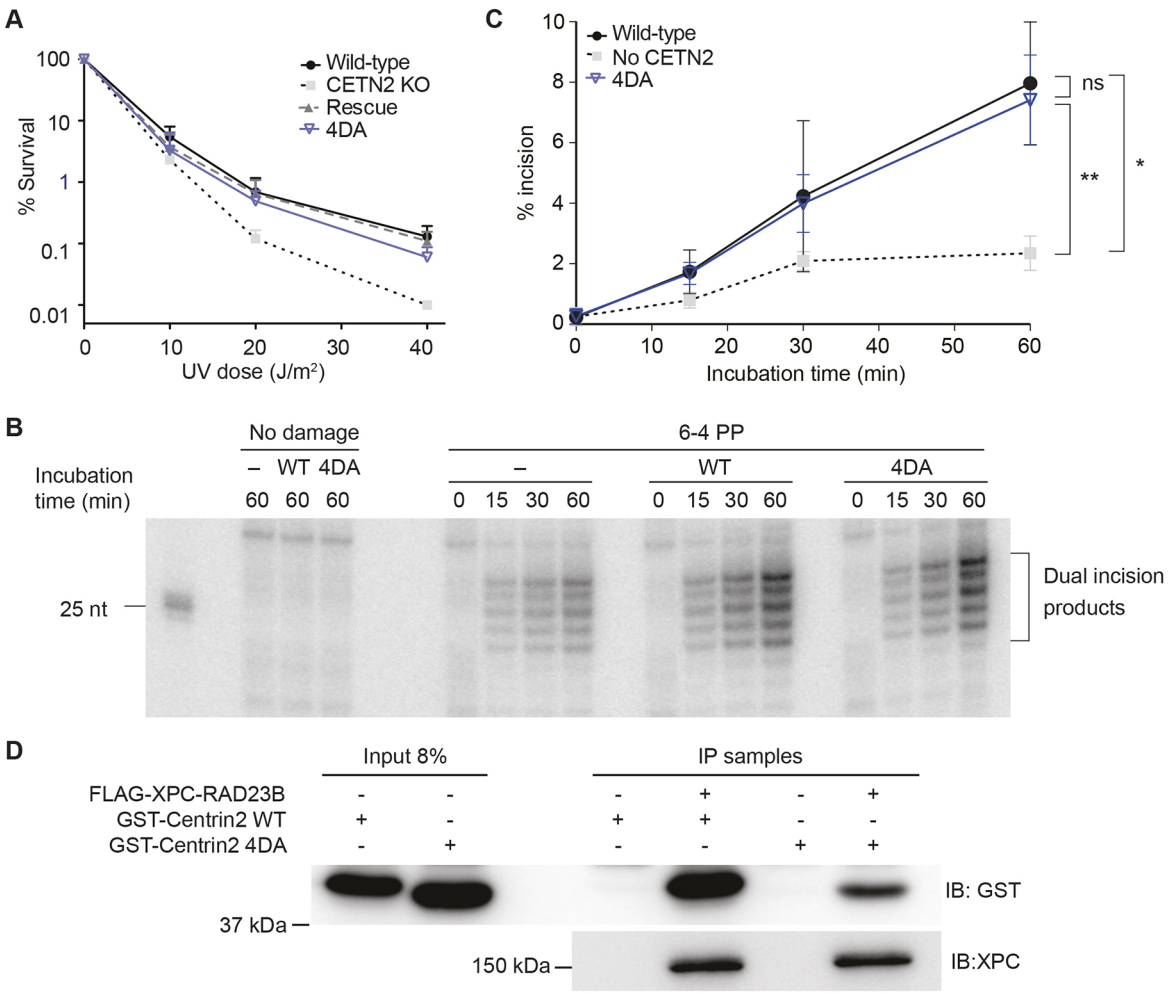

Fig. 2. Centrin 2 EF-hand mutants are proficient in NER. (A) Clonogenic survival of cells of the indicated genotypes after exposure to various doses of UV irradiation. Data points represent the percentage survival (mean±s.d.) from three separate experiments. (B) *In vitro* NER dual incision assays with DNA containing a 6-4 photoproduct (6-4 PP) or undamaged control DNA in the presence of XPC–RAD23B complex and the indicated form of centrin 2 (–, no centrin 2 control). (C) Quantitative analysis of the *in vitro* dual incision products. Percentage incision (mean±s.d.) was calculated from three independent experiments. ns, not significant; **P*<0.05, ***P*<0.01 by two-way ANOVA. (D) *In vitro* binding experiment showing the binding of purified recombinant XPC–RAD23B complex to recombinant wild-type and 4DA centrin 2 proteins.

PCM1 levels around the centrosome, similar to that seen in the *CETN2* null clone (Fig. 3A,B). This observation suggests a role for centrin 2 in satellite regulation, consistent with the previously described localization of centrin to satellites (Löffler et al., 2013; Prosser et al., 2009). Alterations in centriolar satellite density can affect centrosome duplication (Flanagan et al., 2017; Kodani et al., 2015; Löffler et al., 2013; Prosser et al., 2009). Therefore, we quantitated centrosome amplification after ionizing (IR) and ultraviolet (UV) irradiation, visualizing centrioles with the proximal end marker CEP135 (Ohta et al., 2002) and centrin 3, which is representative of a distinct family of centrins (Fig. 3C) (Middendorp et al., 2000). *CETN2* mutants showed similar levels of centriole amplification (three or more than four centrioles) as wild-type cells, except in the case of D77A mutants, where there was a moderate reduction (Fig. 3D). In general, *CETN2* mutants showed more cells with two centrioles and fewer with four than controls after IR and UV irradiation, potentially indicating some altered cell cycle distribution. However, IR- and UV-induced phosphorylation of CHK1 and CDK2, modifications that are necessary for DNA damage-induced centrosome amplification (Bourke et al., 2010), were initiated with normal kinetics in centrin 2-deficient and centrin 2 4DA-expressing cells, suggesting that DNA damage-responsive cell cycle checkpoint signaling was unaffected by the loss of centrin 2 or its EF-hands (Fig. S1A,B).

Requirement for the EF-hands of centrin 2 in primary ciliogenesis

Our next question concerned the requirement for centrin 2 EF-hands in primary cilium formation. To address this, we serum-starved the *CETN2* mutant clones and quantitated primary cilium formation by immunofluorescence microscopy of acetylated tubulin, Arl13B and glutamylated tubulin. As shown in Fig. 4A,B, staining for acetylated and glutamylated tubulin recapitulated previous findings in which we observed a marked deficit in primary cilium formation in the absence of centrin 2 (Prosser and Morrison, 2015). None of the EF-hand mutants could rescue primary ciliation, with the D77A and 4DA mutants showing a more severe phenotype than even the null cells. This result was seen in two additional *CETN2* null clones that expressed each mutant, so the impact of D77A and 4DA mutations was not the result of individual clonal effects. A more moderate ciliary defect was seen with ARL13B staining of centrin 2 mutant cells, again with the D77A and 4DA mutants showing a particularly

Journal of Cell Science (2019) 132, jcs228486. doi:10.1242/jcs.228486

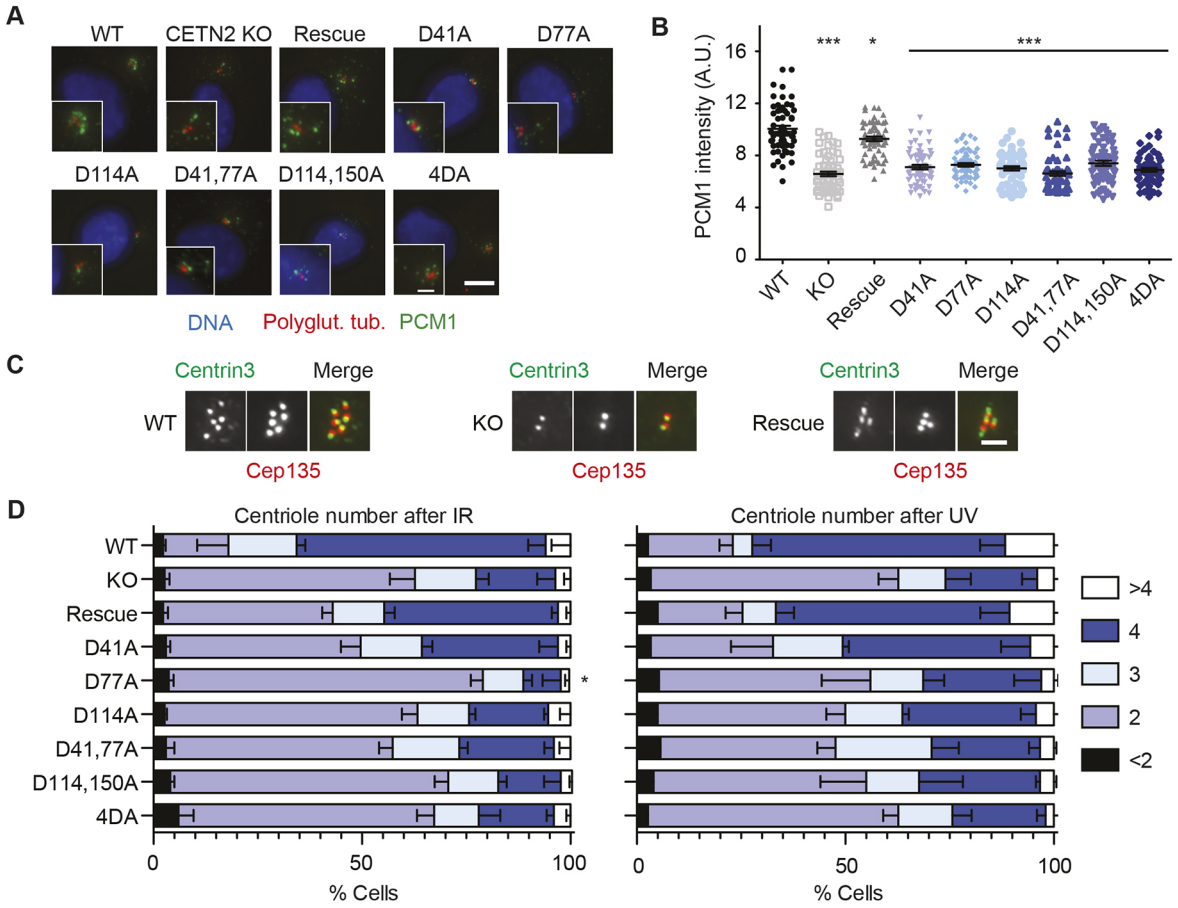

Fig. 3. Centrin 2 and its EF-hand mutants are required for centriolar satellite localization. (A) Immunofluorescence micrograph showing centriolar satellite localization in wild-type cells and the indicated centrin 2 mutant-expressing clones. (B) Quantitation of PCM1 intensity within 30 µm^2 around the polyglutamylated tubulin centrosome signal after 18 h serum starvation. Data show intensity (mean±s.e.m.) in arbitrary fluorescence units (A.U.) determined from 60 cells in two separate experiments. (C) Immunofluorescence micrograph with the centriolar markers Cep135 and centrin 3 to visualize centrosome numbers after 5 Gy ionizing radiation (IR) in wild-type, *CETN2* null and rescue cells. Images of >4, 2 and 4 centrioles are shown. (D) Quantitation of centriole numbers in cells of the indicated genotype 48 h after 5 Gy IR or 5 J/m^2 UV irradiation, scored by microscopy image analysis of Cep135 and centrin 3. Data show percentage (mean±s.d.) of cells with the indicated number of centrosomes from three separate experiments in which at least 100 cells were quantitated. The percentage of cells with centriole amplification (3 or >4) was compared with the percentage in control cells. **P*<0.05, ****P*<0.001 compared with wild type by one-way ANOVA and Dunnett's multiple comparison test. Scale bars: 5 µm (A); 2 µm (A inset, C).

clear deficiency. As the ARL13B signal reveals the membrane region around the extension of an axoneme, these observations are consistent with compromised stability of the tubulin-based axonemal structure in centrin 2 mutants, within an ARL13B-containing ciliary membrane. Notably, those few centrin 2 null, D77A and 4DA cells that did make a cilium were markedly deficient in ciliary Hedgehog signaling, with a significantly reduced number of cells being capable of relocalizing Smoothened to the cilium in response to agonist stimulation (Fig. 4C,D). These findings suggest that changes in the EF-hands of centrin strongly affect ciliary integrity and dynamics, as determined by tubulin stability within cilia and by ciliary functioning.

Causes of the ciliary defect seen in the absence of centrin 2 include the improper retention of CP110 at the distal end of the mother centriole and the defective localization of TTBK2 (Prosser and Morrison, 2015). To test whether CP110 regulation was affected by mutation of centrin 2 EF-hands, we scored CP110 localization in serum-starved cells and found that mutation of any of the EF-hands impaired CP110 removal after serum starvation, to at least the same extent as observed in *CETN2* null cells (Fig. 5A,B). A key regulator of appropriate TTBK2 localization is the distal appendage protein CEP164 (Cajanek and Nigg, 2014; Oda et al., 2014). We used STORM microscopy to visualize CEP164 structures in centrin 2-deficient cells and in cells that lacked centrobin, another centriolar component whose absence negatively affects CP110 removal and primary ciliogenesis (Betzig et al., 2006; Heilemann et al., 2008; Rust et al., 2006; Yang et al., 2018; Ogungbenro et al., 2018). As shown in Fig. 5C,D, CEP164 formed ninefold patterns with similar radii in wild-type, centrin 2 null, centrobin null and 4DA cells, suggesting that the distal appendage structures are unaffected by the absence of centrin 2 or centrobin, or by the mutation of the EF-hands of centrin 2 (Tanos et al., 2013; Yang et al., 2018). We then monitored TTBK2 localization to mother centrioles and found that cells expressing any of the EF-hand mutants were compromised in localizing TTBK2 to the centriole after serum starvation to the same extent as null cells (Fig. 5E,F). STORM imaging revealed a marked distortion of TTBK2 in centrin 2-deficient cells (Fig. 5G,H). Given the abnormal localization of CEP164 away from the appendages that we have previously noted in *CETN2* null cells (Prosser and Morrison, 2015), these findings show that the localization of CEP164 to the distal appendages is not sufficient to ensure appropriate TTBK2 localization. Furthermore, our observations implicate all four of the

Journal of Cell Science (2019) 132, jcs228486. doi:10.1242/jcs.228486

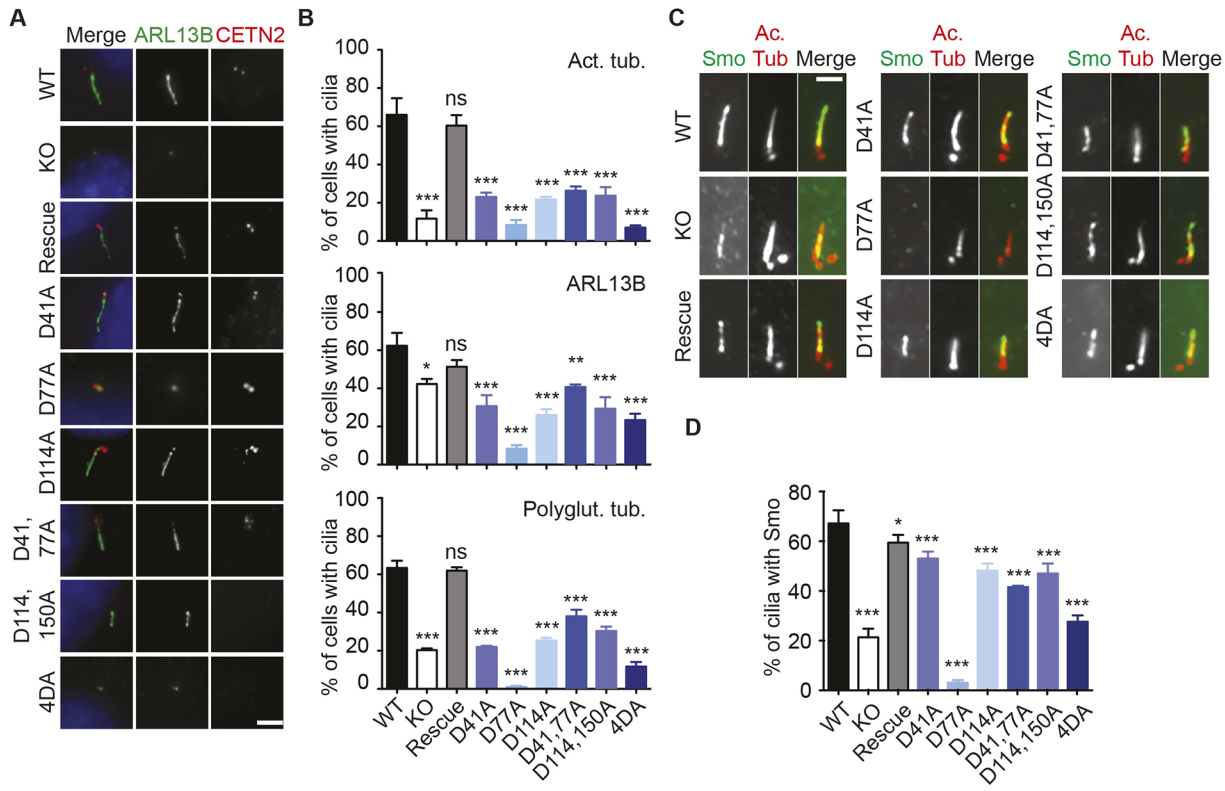

Fig. 4. Defective ciliogenesis and ciliary function in centrin 2-deficient and EF-hand mutant cells. (A) Immunofluorescence micrograph showing representative images of ciliary structures observed in cells of the indicated genotype after 18 h serum starvation. (B) Percentage (mean±s.e.m.) of cells with cilia after 18 h serum starvation, as determined by staining for the indicated ciliary marker, scored from three separate experiments in which at least 100 cells were counted. (C) Immunofluorescence micrograph showing Smo localization to the cilium in cells of the indicated genotype. Cells were serum-starved for 48 h and then treated with 100 nM SAG for 4 h prior to fixation and analysis. (D) Percentage (mean±s.e.m.) of ciliated cells with Smo localization to the cilium, scored from three separate experiments in which at least 30 cilia were counted. ns, not significant; **P*<0.05, ***P*<0.01, ****P*<0.001 compared with wild type by one-way ANOVA and Dunnett's multiple comparison test. Scale bars: 5 µm (A); 2 µm (C).

EF-hands of centrin 2 in the regulation of CP110 removal and TTBK2 localization to the distal end of the mother centriole.

Our findings suggest defects in tubulin stability or transport during ciliogenesis in centrin 2 mutant cells, rather than problems in vesicle docking (Fig. 4A,B, Fig. 5) (Prosser and Morrison, 2015). Therefore, we tested whether the length of cilia was affected in centrin 2 mutant cells by staining cells with antibodies against acetylated tubulin. We found that in those centrin 2-deficient and D77A cells that made cilia, the cilia were shorter than those seen in wild-type and rescued null cells; 4DA cells showed slightly longer cilia than controls (Fig. 6A,B). To test the notion that centrin 2 levels might affect tubulin stabilization, we overexpressed centrin 2 in wild-type and *CETN2* null cells and measured the length of cilia observed after 18 h serum starvation. We found that cilia were significantly longer in the cells where centrin 2 was expressed in addition to the endogenous amount (Fig. 6C,D). These findings indicate a role for centrin 2 in controlling the extension and stabilization of the axoneme.

A number of centrin functions have been ascribed to its assembly of multimeric structures, including self-aggregation (Wiech et al., 1996; Azimzadeh et al., 2009; Kilmartin, 2003; Martinez-Sanz et al., 2006). The accessibility of the binding regions on centrin 2 to interacting peptide sequences depends on structural shifts induced by calcium binding, with different calcium-dependent effects seen in different species (reviewed in Dantas et al., 2012; Zhang and He, 2011). To explore how centrin interactions are affected by the calcium-binding capacity of the EF-hands, we performed immunoprecipitation experiments with centrin 2 and the 4DA mutant form. As shown in Fig. 7, centrin 2 co-immunoprecipitated with both SFI1 and POC5 from human TERT-RPE1 cells, although with a diminishing amount of both following serum starvation. These interactions required centrin 2 and were dependent on its EF-hands, although a potential caveat lies in the reduced level of the 4DA form of centrin 2 that we precipitated in this experiment, similar to results seen with the XPC interaction. These observations show that a marked defect in centrin 2-containing complex assembly results from the loss of EF-hand function, which is consistent with a model in which centrin 2 multimerization contributes to primary ciliogenesis.

DISCUSSION

In this study, we examined the requirement for the EF-hand domains of human centrin 2 in primary ciliogenesis and NER and found a distinct separation between the functional requirements for these two activities of the protein. Although mutagenesis of individual EF-hands still allowed the centrosome localization of centrin 2, we saw a marked impact on ciliogenesis when even a single EF-hand was disrupted, resulting in problems with axonemal extension or stabilization, localization of TTBK2 to apparently intact distal appendages, removal of CP110 and centriolar satellite dynamics. These defects were independent of the localization of centrin 2 to the centriolar distal lumen, as we observed them in individual EF-hand mutants that localized to centrioles, as well as in the 4DA mutant, which did not. Nevertheless, *in vitro* NER activity was intact even in experiments that used only the 4DA mutant form of centrin 2, in

Journal of Cell Science (2019) 132, jcs228486. doi:10.1242/jcs.228486

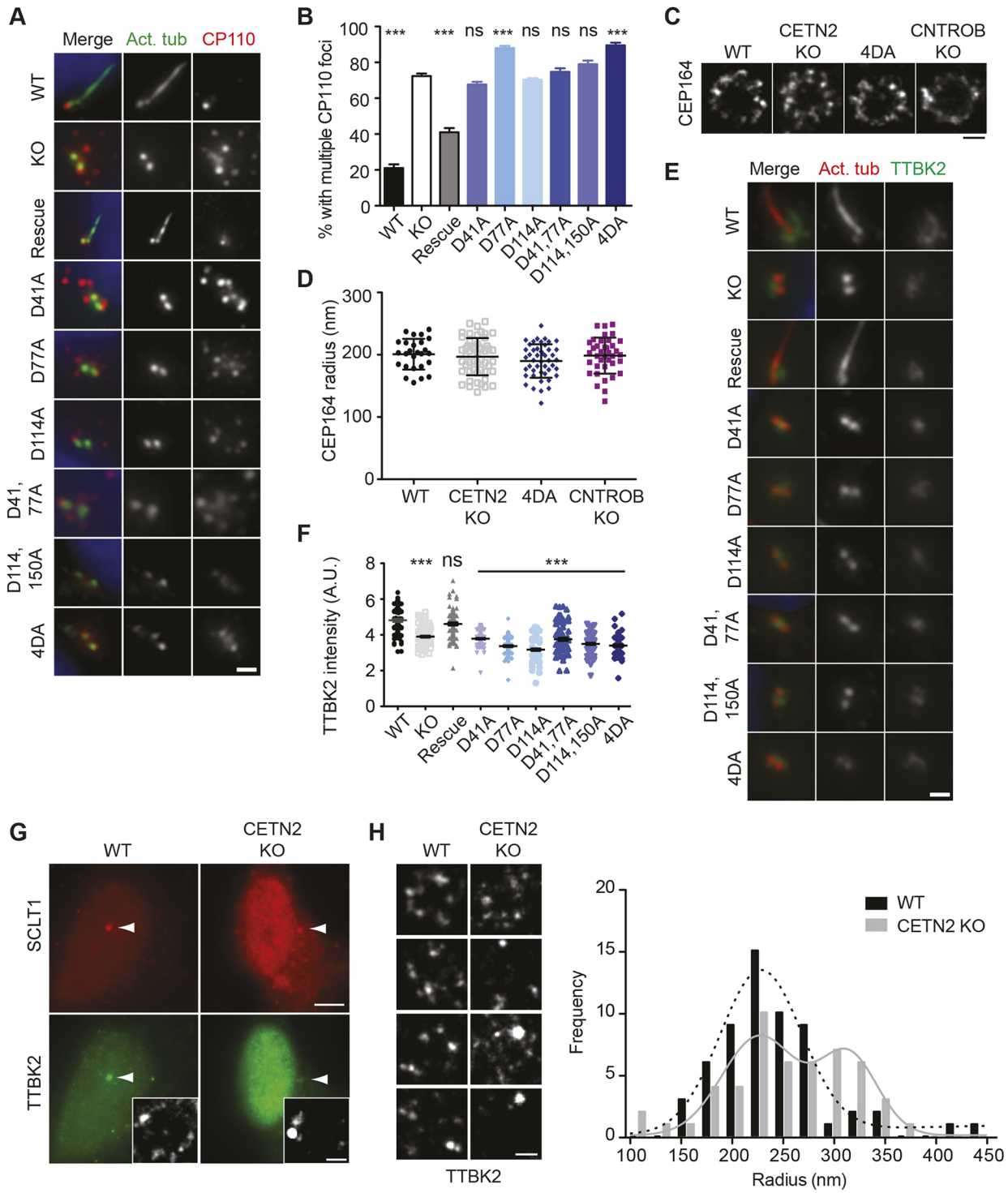

Fig. 5. Centrin 2 and its EF-hands are required for efficient removal of CP110 and appropriate localization of TTBK2. (A) Immunofluorescence micrographs showing representative images of CP110 localization (red) around centrioles (green; acetylated tubulin, Act. tub.) in cells of the indicated genotype after 18 h serum starvation. (B) Percentage (mean±s.e.m.) of cells with multiple CP110 foci around centrioles after 18 h serum starvation, scored from three separate experiments in which at least 100 cells were counted. (C) Representative dSTORM images showing the annular structures formed by CEP164 in cells of the indicated genotype. (D) Frequency plots of the radius (mean±s.d.) of the CEP164 rings visualized by dSTORM in cells of the indicated genotype, from at least 27 data points out of 3–4 centrioles. (E) Immunofluorescence micrographs of TTBK2 (green) localization around centrioles/basal bodies (red). (F) Dot plots of TTBK2 intensity measurements within a 30 μm^2 area around the centrosome. Plot shows data in arbitrary units (A.U.) from three separate experiments in which 30 individual cells of the indicated genotype or centrin 2 transgene expression were analyzed. (G) Immunofluorescence microscopy analysis of TTBK2 (green), with Sclt1 (red) to confirm axial orientation of the centriole (arrows), in hTERT-RPE1 cells of the indicated genotype after 24 h serum starvation. dSTORM axial views of TTBK2 are shown in the insets. (H) Left: dSTORM images show the distribution patterns of TTBK2 in hTERT-RPE1 and centrin 2 null cells after 24 h serum starvation. Right: Frequency distribution of the TTBK2 signal radius around Sclt1 in centrin 2-deficient cells implies that TTBK2 is located in a more dispersed and random manner in the absence of centrin 2. ns, not significant; ***P<0.001 compared with wild type by one-way ANOVA and Dunnett's multiple comparison test. Scale bars: 2 µm (E); 2.5 µm (A); 5 µm (G); 200 nm (C,G inset, H).

Journal of Cell Science (2019) 132, jcs228486. doi:10.1242/jcs.228486

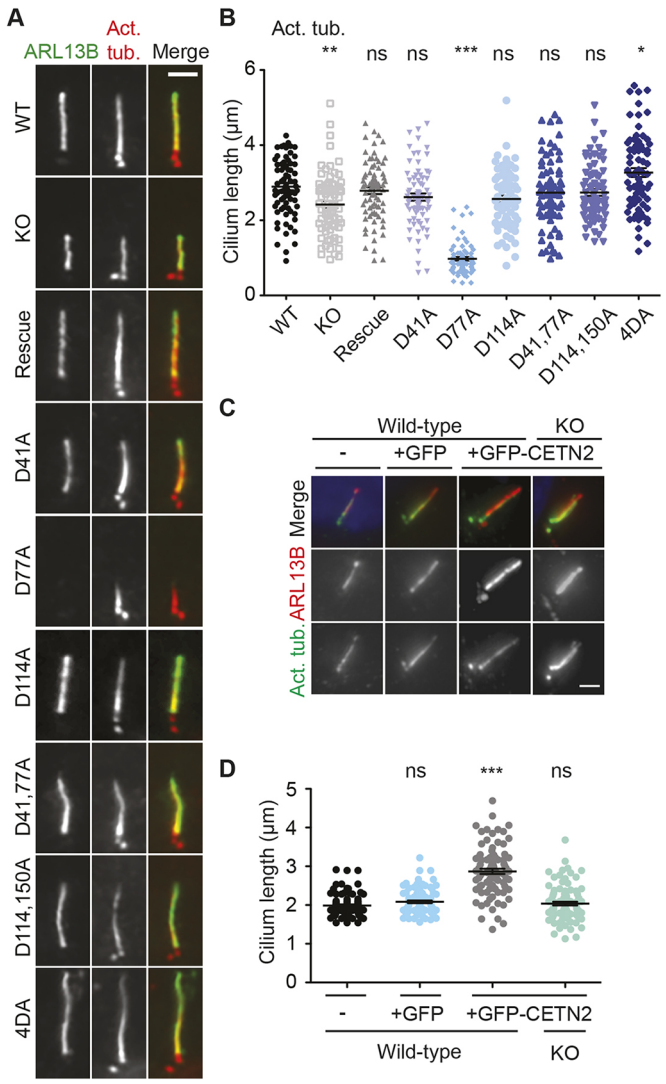

Fig. 6. Centrin 2 and its EF-hands affect primary cilium length. (A) Immunofluorescence microscopy analysis of cilia using the indicated markers in cells of the indicated genotype. (B) Cilium length (mean±s.d.) from three independent experiments in which cilia were measured in 30 cells after 24 h serum starvation using acetylated tubulin as a ciliary axoneme marker. (C) Immunofluorescence microscopy analysis of cilia in cells transfected with the indicated GFP expression construct 24 h prior to 18 h serum starvation. (D) Cilium length (mean±s.d.) from three independent experiments in which cilia were measured in 30 cells using ARL13B as a ciliary axoneme marker. ns, non-significant; **P*<0.05, ***P*<0.01, ****P*<0.001 compared with wild type by one-way ANOVA and Dunnett's multiple comparison test. Scale bars: 2 µm (A,C).

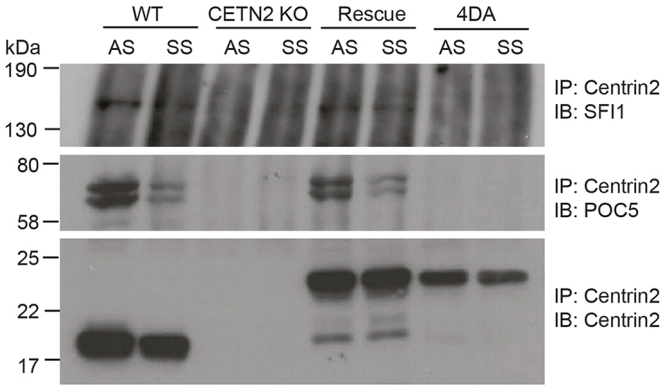

Fig. 7. EF-hand-dependent interaction of centrin 2 with POC5 and SFI1. Lysates from wild-type and *CETN2* null cells with or without the indicated centrin 2 transgene were immunoprecipitated (IP) with antibodies to centrin 2 and blotted with antibodies to the indicated protein (IB).

which all 4 EF-hands had been mutated. Furthermore, clonogenic survival after UV irradiation was normal in cells that expressed the 4DA mutant. We observed an analogous result in chicken DT40 cells, where the 4DA mutant was also defective in centriole localization but was capable of allowing wild-type levels of survival after UV irradiation in a clonogenic survival assay (Dantas et al., 2013). The contrasting phenotypic data with respect to these two functions of centrin 2 suggest that each of the EF-hands specifies a key activity of centrin 2 in ciliogenesis or that the structural changes imposed by mutation of any of the EF-hands abrogate a centrosomal or ciliary function of human centrin 2 that is dispensable in NER.

A model for centrin function is that calcium binding allows the protein to interact with target peptides, with calcium mediating a switch to a higher-affinity state of the protein for specific binding partners, as in the case of *Chlamydomonas* centrin and a Kar1 peptide (Veeraraghavan et al., 2002; Ortiz et al., 2005; Hu et al., 2004) or yeast Cdc31p and a Kar1p peptide (Geier et al., 1996). Work with *Scherffelia dubia* centrin and human peptides found that low-affinity N-terminal peptide binding sites became activated in the presence of calcium (Radu et al., 2010), although the extent to which the XPC peptide binding in that study is relevant could be questionable, given our findings on the NER capacity of the 4DA mutant. *In vitro* data have indicated that the high-affinity calcium-binding sites of human centrin1 and centrin 2 lie in the C-terminal EF-hands, with the N-terminal EF-hands being of lower affinity and responding to the calcium occupancy status of the C-terminal sites (Durussel et al., 2000; Matei et al., 2003; Yang et al., 2006; Nishi et al., 2013). Interestingly, analysis of the crystal structure of the homologous mouse centrin1 protein suggests that calcium occupancy of the N-terminal EF-hands facilitates centrin1 dimerization through structural alterations that occur upon binding of each of the four EF-hands (Kim et al., 2017). Although these observations imply that a hierarchy of calcium affinities determines the roles of individual EF-hands in centrin functions, we observed relatively little phenotypic distinction between the individual EF-hand mutants, the 4DA mutant and the centrin 2 null cells in terms of ciliation. Unexpectedly, we saw a marked impact of the D77A mutation, one of the N-terminal EF-hands. However, the D41,77A double mutant showed a less dramatic phenotype and so it is unclear how this specific mutant impacts on centrin 2 activities.

Previous analyses have demonstrated that centrin forms large aggregates with both itself and its interactors, such as XPC (Araki et al., 2001), Kar1p (Spang et al., 1995), Sfi1p (Kilmartin, 2003) and CP110 (Tsang et al., 2006). Several studies have demonstrated the importance of calcium binding in self-aggregation of centrins from multiple species (Wiech et al., 1996; Tourbez et al., 2004; Yang et al., 2006; Li et al., 2006; Wang et al., 2018), as well as in the assembly of multimeric complexes with Sfi1p (Kilmartin, 2003; Li et al., 2006; Martinez-Sanz et al., 2006). Our data clearly indicate the need for calcium binding capacity in allowing the assembly of human centrin 2–SFI1–POC5 complexes, consistent with previous observations we made on the requirement for centrin in the assembly of POC5 aggregate structures (Dantas et al., 2013). POC5 is required for centriole elongation, although its role is not yet understood (Azimzadeh et al., 2009). Overexpressed POC5 can assemble into linear aggregates in a centrin-dependent manner (Dantas et al.,

Journal of Cell Science (2019) 132, jcs228486. doi:10.1242/jcs.228486

2013). SFI1p–Cdc31p filament assembly is necessary for spindle pole duplication in budding yeast, potentially providing a scaffold for extension of the half-bridge (Li et al., 2006). Although control of SFI1–centrin filament dynamics through calcium-regulated changes in centrin conformation has been proposed as a contractility mechanism (Kilmartin, 2003) and demonstrated by analysis of infraciliary lattice contractility in *Paramecium tetraurelia* (Gogendeau et al., 2007), it is not clear how this affects extension of the primary cilium in human cells. *In vitro* analyses of the impact of calcium chelation on the assembly of this complex showed little effect with the yeast proteins, but a reduction with the human centrin 2 protein (Kilmartin, 2003). Together, these data indicate that SFI1 and POC5 are assembled into larger complexes that involve centrin 2, although the phenotypic impact of the loss of such complexes in the absence of functional centrin 2 remains to be defined.

We also noted that centrin 2 loss or calcium-binding deficiency impacted on centriolar satellite aggregation, as measured by PCM1 signal. Centriolar satellites have been suggested to act as regulators of centrosome duplication by controlling availability of centrosome components (Dammermann and Merdes, 2002; Kubo and Tsukita, 2003; Firat-Karalar et al., 2014; Tollenaere et al., 2015) and more recent data have similarly implicated them in ciliogenesis (Odabasi et al., 2019; Quarantotti et al., 2019). The reduction of ciliogenesis in cells deficient in centrin 2 or expressing an EF-hand mutant might thus reflect deficient aggregation of centrosome regulators in centriolar satellites.

An alternative explanation for the defects in ciliogenesis that we observed here is instability in axonemal tubulin structures in the absence of centrin or its EF-hands. Such an idea would be consistent with the reduced ciliation frequency and length, as determined by measurement with tubulin markers, and the more limited impact seen when ARL13B was used as a marker. In support of this notion are the basal body stability defects described in *Tetrahymena* upon deletion or mutagenesis of the C-terminal EF-hands of Cen1, the principal centrin 2 ortholog in that organism (Stemm-Wolf et al., 2005; Vonderfecht et al., 2011). This model suggests that centrin contributes to ciliogenesis by regulating dynamic protein assemblies at the distal end of the centrioles. However, the mechanism by which centrin can affect tubulin assembly in ciliogenesis is unclear. A proteomic study of the interactions of centriolar proteins did not describe centrin as a tubulin interactor (Gupta et al., 2015), so such regulation could be indirect. Given the effects that centrin deficiency or EF-hand mutagenesis have on key aggregate structures, CP110 is an attractive candidate for mediating centrin functions in ciliogenesis. CP110 is a negative regulator of centriole length and its depletion facilitates microtubule extension, although additional activities are necessary for ciliogenesis proper (Schmidt et al., 2009; Spektor et al., 2007). CP110 can be co-immunoprecipitated with centrin and co-fractionates with it in large (megadalton) complexes (Tsang et al., 2006). Centrin 2-dependent removal of CP110 from the distal end of the centriole is necessary for primary ciliogenesis (Prosser and Morrison, 2015). As TTBK2 localization is also required for the correctly regulated removal of CP110 (Cajanek and Nigg, 2014; Oda et al., 2014), CP110 dynamics might be controlled by centrin through interactions in larger complexes, potentially in centriolar satellites (Tsang and Dynlacht, 2013), or through TTBK2 regulation at the distal end of the centriole. A remaining question is whether POC5 and SFI1 play any role in these processes. The availability of NER-competent, ciliation-defective centrin 2 mutants will allow dissection of the interactions of centrin in these activities.

MATERIALS AND METHODS

Cell culture

Human TERT-RPE1 cells were obtained from ATCC and grown in DMEM-F12 medium with 10% fetal bovine serum and 1% penicillin-streptomycin in a humidified 5% CO_2 atmosphere at 37°C. *CETN2* knockout clones were generated in a previous study (Prosser and Morrison, 2015). Mycoplasma testing was performed every 2 months. Transfections were performed using Lipofectamine 2000 (Thermo Fisher) as per the manufacturer's instructions. For stable transfections, cells were trypsinized 18 h post-transfection and serial dilutions were performed into medium containing 1 mg/ml G418 (Invitrogen). Cells were placed under selection for 7–14 days, after which colonies were lifted using cloning discs (Sigma-Aldrich). Serum starvation conditions consisted of DMEM-F12 medium with 0.1% FBS. SAG (EMD Millipore) was used on cells at 100 nM, prepared from a 1 M stock made up in DMSO. Irradiations were performed using a ^{137}Cs source at 9.5 Gy/min (Mainance Engineering) or with an NU-6 254 nm UV-C lamp at 23/m^2/min (Benda). UV clonogenic survival assays were performed as previously described (Daly et al., 2016).

Cloning and molecular biology

Human *CETN2* cDNA sequence (Inanç et al., 2010) was cloned into pCMV-3tag-Myc (Agilent). Site-directed mutagenesis was performed using a Quick-Change II XL kit (Agilent) following the manufacturer's instructions with the following primer pairs: centrin 2 D41A (forward) 5′-CCGGGAAGCTTTTGATCTTTTCGCTGCGGATGGAACTGGCAC-CATAGATG-3′; (reverse) 5′-CATCTATGGTGCCAGTTCCATCCGCA-GCGAAAAGATCAAAAGCTTCCCGG-3′; centrin 2 D77A (forward) 5′-TAAGAAAATGATAAGTGAAATTGCTAAGGAAGGGACAGGAA-AAATGAA-3′; (reverse) 5′-TTCATTTTTCCTGTCCCTTCCTTAGCAA-TTTCACTTATCATTTTCTTA-3′; centrin 2 D114A (forward) 5′-AATCCTGAAAGCTTTCAAGCTCTTTGCTGATGATGAAACTGG-GAAGATT-3′; (reverse) 5′-AATCTTCCCAGTTTCATCATCAGCAAA-GAGCTTGAAAGCTTTCAGGATT-3′; centrin 2 D150A (forward) 5′-CTGCAGGAAATGATTGATGAAGCTGCTCGAGATGGAGATGGAG-AGGTC-3′; (reverse) 5′-GACCTCTCCATCTCCATCTCGAGCAGCTT-CATCAATCATTTCCTGCAG-3′. Each single mutant was generated and additional rounds of mutagenesis performed subsequent to DNA sequence verification of the individual mutation (Source Biosciences). For bacterial expression, centrin 2-encoding sequences were subcloned into the *Bam*HI-*Xho*I sites of pGEX-4T (GE Healthcare). For RT-PCR, cDNA synthesis was performed using a High-Capacity RNA to cDNA kit (Agilent) and PCR using KOD Hot Start (Applied Biosystems), according to the manufacturers' instructions.

Immunoblotting

Whole-cell extracts were prepared with radioimmunoprecipitation assay buffer (50 mM Tris-HCl pH 7.4, 1% NP-40, 0.25% sodium deoxycholate, 150 mM NaCl, 1 mM EDTA, with protease and phosphatase inhibitor cocktails). Blots were detected by ECL (GE Healthcare). The following primary antibodies were used: rabbit polyclonals against centrin 2 (1:1000; 15877-1-AP, Proteintech), phosphorylated CDK2 T160 (1:500; 2561, Cell Signaling Technology), POC5 (1:500; A303-340A, Bethyl), SFI1 (1:400; 13550-1-AP, Proteintech); rabbit monoclonals against GAPDH (1:5000; 14C10, Cell Signaling Technology), phosphorylated CHK1 S345 (1:1000; 133D3, Cell Signaling Technology) and mouse monoclonals against CDK2 (1:1000; D12, Santa Cruz Biotechnology), CHK1 (1:500; DCS310, Sigma-Aldrich). HRP-conjugated goat anti-mouse or anti-rabbit secondary antibodies were used at 1:5000 (Jackson ImmunoResearch Laboratories).

Immunoprecipitation

Whole-cell extracts were prepared in immunoprecipitation (IP) lysis buffer (50 mM Tris HCl pH 7.4, 150 mM NaCl, 1 mM EDTA pH 8.0, 20% glycerol, 0.5% sodium deoxycholate, 1% IGEPAL CA-630) with protease inhibitor cocktail and 1:1000 dilution of benzonase (Sigma-Aldrich) added fresh before use. Samples were incubated with rotation for 60 min at 4°C, then centrifuged for 20 min at 13,200 ***g*** at 4°C. Supernatants were transferred to fresh Eppendorf tubes. Protein A/G beads (Santa Cruz Biotechnology) were washed three times with IP lysis buffer, then incubated with primary

antibody for 2 h at 4°C. Bead–antibody complexes were washed three times with IP lysis buffer and incubated with 1–2 mg total cell extracts overnight at 4°C on a rotating wheel. Beads were then spun down at 250 ***g*** for 5 min and the supernatant discarded, after which the bead-bound proteins were washed five times in IP lysis buffer prior to boiling in sample buffer.

Expression of recombinant proteins in *E. coli*

Glutathione S-transferase (GST) fusion proteins were expressed in *Escherichia coli* BL21-CodonPlus-RIL by induction with 1 mM IPTG for 3 h. Cell pellets were resuspended in TEN buffer (10 mM Tris-Cl pH 8.0, 1 mM EDTA, 100 mM NaCl) supplemented with protease inhibitors, and then disrupted by sonication. The lysates were centrifuged for 30 min at 200,000 ***g*** at 2°C. The clarified extracts were loaded onto a GSTrap HP column (GE Healthcare) equilibrated with TEN-T buffer (TEN buffer containing 0.1% Triton X-100). After extensive washing with TEN-T buffer, bound proteins were eluted using GST elution buffer (20 mM Tris-HCl pH 8.4; 0.1 M NaCl; 0.1% Triton X-100; 20 mM glutathione). Eluates were dialyzed against buffer containing 50 mM Tris-HCl, pH 8.0, and 10 mM $CaCl_2$, added to washed Thrombin CleanCleave beads (Sigma-Aldrich), and rotated overnight at room temperature. After removal of the beads by passing through disposable plastic columns (Thermo Fisher), the samples were loaded onto a RESOURCE Q column (GE Healthcare), which was tandemly connected to a GSTrap HP pre-column and equilibrated with buffer Q (50 mM Tris-HCl pH 8.0; 1 mM DTT). After extensive washing with buffer Q, the pre-column was disconnected and protein bound to the RESOURCE Q column was eluted with a linear NaCl gradient (0–0.5 M) in buffer Q. Finally, the peak fractions were further purified with size exclusion chromatography with a Superdex 75 column (GE Healthcare) equilibrated with 1×PBS.

In vitro protein interaction and NER assays

Anti-FLAG magnetic beads (Wako) were washed three times in XPC dilution buffer (20 mM Na-phosphate, pH 7.8; 10% glycerol; 1 mM EDTA; 0.3 M NaCl; 1 mM DTT) then incubated in 100 µl of the same buffer containing 200 ng of FLAG–XPC–RAD23B–His complex and 20 µg of acetylated BSA for 2 h at 4°C with stirring. The beads were then washed three times with XPC dilution buffer and incubated with 300 ng of GST–centrin 2 in 100 µl of XPC dilution buffer containing 20 µg of acetylated BSA for 2 h at 4°C with stirring. The beads were then washed nine times with XPC dilution buffer. Bound complexes were competed off by the addition of 40 µl of 0.5 mg/ml FLAG peptide, which was stirred at 4°C for 3 h before the beads were removed by magnet and the samples prepared for polyacrylamide gel electrophoresis (PAGE).

In vitro NER dual incision assays were carried out with purified NER proteins and internally ^{32}P-labeled DNA substrate with or without a single 6-4 photoproduct as previously described (Nishi et al., 2005, 2013). The XPC–RAD23B complex (10 ng) was mixed with 10 ng of centrin 2 (WT or 4DA) and pre-incubated at 4°C for 30 min before being added to the standard reaction mixture. After incubation at 30°C for various time periods, DNA samples were purified and subjected to denaturing PAGE. Dried gels were exposed to BAS imaging plates (Fujifilm) and analyzed with Typhoon FLA 9500 scanner and ImageQuant TL software (GE Healthcare).

Microscopy

Human TERT-RPE1 cells were grown on sterile glass coverslips and fixed in methanol plus 5 mM EGTA at −20°C for 10 min. For microscopy after staining with acetylated or detyrosinated tubulin, cells were incubated on ice for 35 min to depolymerize the microtubule cytoskeleton before fixation. Cells were blocked in 1% BSA before 1 h incubation with primary antibodies and 45 min incubation with Alexa Fluor 488- or 594-labeled donkey secondary antibodies (Invitrogen). Mouse monoclonal antibodies used were as follows: acetylated tubulin (1:1000; 6-11B-1, Sigma-Aldrich), γ-tubulin (1:200; GTU88, Sigma-Aldrich), centrin 2 (1:1000; 20H5, Millipore), centrin 3 (1:1000; 3E6, Abnova), CEP164 (1:10,000; 1F3G10) (Daly et al., 2016), polyglutamylated tubulin (1:500; GT335, Adipogen). Rabbit polyclonal antibodies used were against Arl13b (1:1000; 17711-1-AP, Proteintech), centrin 2 (1:1000; 15877-1-AP, Proteintech), CEP135 (1:500; ab75005, Abcam), CEP164 (1:1000; HPA037606, Sigma-Aldrich), CP110 (1:1000; 12780-1-AP, Proteintech), Smoothened (1:500; ab38686, Abcam), TTBK2 (1:500; 15072-1-AP, Proteintech). Goat polyclonal Sc-50164 (Santa Cruz Biotechnology) was used at 1:400. DNA was stained with Hoechst 33258 (Sigma-Aldrich). Coverslips were mounted in 80% (v/v) glycerol in PBS containing 3% (w/v) *N*-propyl-gallate and DAPI.

Fluorescence imaging and counts were performed using an Olympus BX51 microscope (with a Hamamatsu C10600 camera) or IX81 microscope (Hamamatsu C4742-80-12AG camera), using a 100× oil (NA 1.35) objective. Serial *z*-sections were taken, merged and saved using Photoshop CS4 (Adobe Systems). Merges and individual channel images were exported as TIFFs for publication. Volocity analysis software v6.2.1 (Perkin-Elmer) was used for signal intensity measurements, in which deconvolved maximum-intensity projections collapsed the 3D volumes into 2D images for determination of fluorescence intensity within a 25 µm^2 circle around each centriole.

dSTORM imaging was performed as previously described in detail (Yang et al., 2018). Briefly, rat polyclonal anti-SCLT1 (1:250) (Tanos et al., 2013), rabbit anti-CEP164 (1:2000; 45330002, Novus Biologicals) and rabbit anti-TTBK2 (1:500; 15072-1-AP, Proteintech) were used as primary antibodies. Alexa Fluor 647 (anti-rabbit A21245, Thermo Fisher) and Cy3B-conjugated secondary antibody (1:100) (Yang et al., 2018) were used as secondary antibodies. Imaging was performed with an Evolve 512 Delta EMCCD camera (Photometrics), a 637 nm laser (OBIS 637 LX 140 mW, Coherent), a 561 nm laser (Jive 561 150 mW, Cobolt) and a 405 nm laser (OBIS 405 LX 100 mW, Coherent), connected to a modified inverted microscope (Eclipse Ti-E, Nikon) using a 100Å 1.49 numerical aperture oil-immersion objective (CFI Apo TIRF, Nikon). Image analysis was performed with the MetaMorph Super-Resolution module (Molecular Devices).

Statistical analysis

Statistical analyses were performed with Prism v5.0 (GraphPad).

Competing interests

The authors declare no competing or financial interests.

Author contributions

Conceptualization: C.G.M.; Formal analysis: E.M.K., S.L.P., H.T., W.M.C., J.-C.L., K.S., C.G.M.; Investigation: E.M.K., S.L.P., H.T., W.M.C., C.G.M.; Writing - original draft: C.G.M.; Writing - review & editing: E.M.K., S.L.P., W.M.C., J.-C.L., K.S.; Supervision: J.-C.L., K.S., C.G.M.; Project administration: J.-C.L., K.S., C.G.M.; Funding acquisition: J.-C.L., K.S., C.G.M.

Funding

This work was funded by Science Foundation Ireland International Strategic Cooperation Award 13/ISCA/2846 and European Commission Seventh Framework Programme SEC-2009-4.3-02, project 242361 'BOOSTER'. E.M.K. received a Ministry of Higher Education King Abdullah Foreign Scholarship. S.L.P. was the recipient of a European Union Horizon 2020 Marie Skłodowska-Curie Global Fellowship (No. 702601). W.M.C. was supported by Academia Sinica, Taiwan grant AS-CDA-104-M06. J.-C.L. was supported by the Ministry of Science and Technology, Taiwan grant 107-2313-B-001-009. This work was supported by Japan Society for the Promotion of Science KAKENHI grant number JP16H06307 to K.S.

Supplementary information

Supplementary information available online at
http://jcs.biologists.org/lookup/doi/10.1242/jcs.228486.supplemental

References

Acu, I. D., Liu, T., Suino-Powell, K., Mooney, S. M., D'assoro, A. B., Rowland, N., Muotri, A. R., Correa, R. G., Niu, Y., Kumar, R. et al. (2010). Coordination of centrosome homeostasis and DNA repair is intact in MCF-7 and disrupted in MDA-MB 231 breast cancer cells. *Cancer Res.* **70**, 3320-3328. doi:10.1158/0008-5472.CAN-09-3800

Araki, M., Masutani, C., Takemura, M., Uchida, A., Sugasawa, K., Kondoh, J., Ohkuma, Y. and Hanaoka, F. (2001). Centrosome protein centrin 2/caltractin 1 is part of the xeroderma pigmentosum group C complex that initiates global genome nucleotide excision repair. *J. Biol. Chem.* **276**, 18665-18672. doi:10.1074/jbc.M100855200

Azimzadeh, J., Hergert, P., Delouvée, A., Euteneuer, U., Formstecher, E., Khodjakov, A. and Bornens, M. (2009). hPOC5 is a centrin-binding protein

required for assembly of full-length centrioles. *J. Cell Biol.* **185**, 101-114. doi:10.1083/jcb.200808082

Betzig, E., Patterson, G. H., Sougrat, R., Lindwasser, O. W., Olenych, S., Bonifacino, J. S., Davidson, M. W., Lippincott-Schwartz, J. and Hess, H. F. (2006). Imaging intracellular fluorescent proteins at nanometer resolution. *Science* **313**, 1642-1645. doi:10.1126/science.1127344

Bourke, E., Brown, J. A. L., Takeda, S., Hochegger, H. and Morrison, C. G. (2010). DNA damage induces Chk1-dependent threonine-160 phosphorylation and activation of Cdk2. *Oncogene* **29**, 616-624. doi:10.1038/onc.2009.340

Braun, D. A. and Hildebrandt, F. (2017). Ciliopathies. *Cold Spring Harb. Perspect Biol.* **9**, a028191. doi:10.1101/cshperspect.a028191

Cajanek, L. and Nigg, E. A. (2014). Cep164 triggers ciliogenesis by recruiting Tau tubulin kinase 2 to the mother centriole. *Proc. Natl. Acad. Sci. USA* **111**, E2841-E2850. doi:10.1073/pnas.1401777111

Chen, Z., Indjeian, V. B., Mcmanus, M., Wang, L. and Dynlacht, B. D. (2002). CP110, a cell cycle-dependent CDK substrate, regulates centrosome duplication in human cells. *Dev. Cell* **3**, 339-350. doi:10.1016/S1534-5807(02)00258-7

Daly, O. M., Gaboriau, D., Karakaya, K., King, S., Dantas, T. J., Lalor, P., Dockery, P., Kramer, A. and Morrison, C. G. (2016). Gene-targeted CEP164-deficient cells show a ciliation defect with intact DNA repair capacity. *J. Cell Sci.* **129**, 1769-1774. doi:10.1242/jcs.186221

Dammermann, A. and Merdes, A. (2002). Assembly of centrosomal proteins and microtubule organization depends on PCM-1. *J. Cell Biol.* **159**, 255-266. doi:10.1083/jcb.200204023

D'angiolella, V., Donato, V., Vijayakumar, S., Saraf, A., Florens, L., Washburn, M. P., Dynlacht, B. and Pagano, M. (2010). SCF(Cyclin F) controls centrosome homeostasis and mitotic fidelity through CP110 degradation. *Nature* **466**, 138-142. doi:10.1038/nature09140

Dantas, T. J., Wang, Y., Lalor, P., Dockery, P. and Morrison, C. G. (2011). Defective nucleotide excision repair with normal centrosome structures and functions in the absence of all vertebrate centrins. *J. Cell Biol.* **193**, 307-318. doi:10.1083/jcb.201012093

Dantas, T. J., Daly, O. M. and Morrison, C. G. (2012). Such small hands: the roles of centrins/caltractins in the centriole and in genome maintenance. *Cell. Mol. Life Sci.* **69**, 2979-2997. doi:10.1007/s00018-012-0961-1

Dantas, T. J., Daly, O. M., Conroy, P. C., Tomas, M., Wang, Y., Lalor, P., Dockery, P., Ferrando-May, E. and Morrison, C. G. (2013). Calcium-binding capacity of centrin 2 is required for linear POC5 assembly but not for nucleotide excision repair. *PLoS ONE* **8**, e68487. doi:10.1371/journal.pone.0068487

Durussel, I., Blouquit, Y., Middendorp, S., Craescu, C. T. and Cox, J. A. (2000). Cation- and peptide-binding properties of human centrin 2. *FEBS Lett.* **472**, 208-212. doi:10.1016/S0014-5793(00)01452-6

Firat-Karalar, E. N., Rauniyar, N., Yates, J. R., III and Stearns, T. (2014). Proximity interactions among centrosome components identify regulators of centriole duplication. *Curr. Biol.* **24**, 664-670. doi:10.1016/j.cub.2014.01.067

Flanagan, A.-M., Stavenschi, E., Basavaraju, S., Gaboriau, D., Hoey, D. A. and Morrison, C. G. (2017). Centriole splitting caused by loss of the centrosomal linker protein C-NAP1 reduces centriolar satellite density and impedes centrosome amplification. *Mol. Biol. Cell* **28**, 736-745. doi:10.1091/mbc.e16-05-0325

Geier, B. M., Wiech, H. and Schiebel, E. (1996). Binding of centrins and yeast calmodulin to synthetic peptides corresponding to binding sites in the spindle pole body components Kar1p and Spc110p. *J. Biol. Chem.* **271**, 28366-28374. doi:10.1074/jbc.271.45.28366

Geiser, J. R., van Tuinen, D., Brockerhoff, S. E., Neff, M. M. and Davis, T. N. (1991). Can calmodulin function without binding calcium? *Cell* **65**, 949-959. doi:10.1016/0092-8674(91)90547-C

Gifford, J. L., Walsh, M. P. and Vogel, H. J. (2007). Structures and metal-ion-binding properties of the Ca2+-binding helix-loop-helix EF-hand motifs. *Biochem. J.* **405**, 199-221. doi:10.1042/BJ20070255

Goetz, S. C. and Anderson, K. V. (2010). The primary cilium: a signalling centre during vertebrate development. *Nat. Rev. Genet.* **11**, 331-344. doi:10.1038/nrg2774

Goetz, S. C., Liem, K. F., Jr and Anderson, K. V. (2012). The spinocerebellar ataxia-associated gene Tau tubulin kinase 2 controls the initiation of ciliogenesis. *Cell* **151**, 847-858. doi:10.1016/j.cell.2012.10.010

Gogendeau, D., Beisson, J., de Loubresse, N. G., Le Caer, J.-P., Ruiz, F., Cohen, J., Sperling, L., Koll, F. and Klotz, C. (2007). An Sfi1p-like centrin-binding protein mediates centrin-based Ca2+ -dependent contractility in Paramecium tetraurelia. *Eukaryot. Cell* **6**, 1992-2000. doi:10.1128/EC.00197-07

Graser, S., Stierhof, Y. D., Lavoie, S. B., Gassner, O. S., Lamla, S., Le Clech, M. and Nigg, E. A. (2007). Cep164, a novel centriole appendage protein required for primary cilium formation. *J. Cell Biol.* **179**, 321-330. doi:10.1083/jcb.200707181

Gupta, G. D., Coyaud, E., Goncalves, J., Mojarad, B. A., Liu, Y., Wu, Q., Gheiratmand, L., Comartin, D., Tkach, J. M., Cheung, S. W. et al. (2015). A dynamic protein interaction landscape of the human centrosome-cilium interface. *Cell* **163**, 1484-1499. doi:10.1016/j.cell.2015.10.065

Heilemann, M., Van De Linde, S., Schuttpelz, M., Kasper, R., Seefeldt, B., Mukherjee, A., Tinnefeld, P. and Sauer, M. (2008). Subdiffraction-resolution fluorescence imaging with conventional fluorescent probes. *Angew. Chem. Int. Ed. Engl.* **47**, 6172-6176. doi:10.1002/anie.200802376

Hu, H., Sheehan, J. H. and Chazin, W. J. (2004). The mode of action of centrin. Binding of Ca2+ and a peptide fragment of Kar1p to the C-terminal domain. *J. Biol. Chem.* **279**, 50895-50903. doi:10.1074/jbc.M404233200

Inanç, B., Dodson, H. and Morrison, C. G. (2010). A centrosome-autonomous signal that involves centriole disengagement permits centrosome duplication in G2 phase after DNA damage. *Mol. Biol. Cell* **21**, 3866-3877. doi:10.1091/mbc.e10-02-0124

Kilmartin, J. V. (2003). Sfi1p has conserved centrin-binding sites and an essential function in budding yeast spindle pole body duplication. *J. Cell Biol.* **162**, 1211-1221. doi:10.1083/jcb.200307064

Kim, S. Y., Kim, D. S., Hong, J. E. and Park, J. H. (2017). Crystal structure of wild-type centrin 1 from Mus musculus occupied by Ca2. *Biochemistry (Mosc.)* **82**, 1129-1139. doi:10.1134/S0006297917100054

Kleylein-Sohn, J., Westendorf, J., Le Clech, M., Habedanck, R., Stierhof, Y.-D. and Nigg, E. A. (2007). Plk4-induced centriole biogenesis in human cells. *Dev. Cell* **13**, 190-202. doi:10.1016/j.devcel.2007.07.002

Kobayashi, T., Kim, S., Lin, Y.-C., Inoue, T. and Dynlacht, B. D. (2014). The CP110-interacting proteins Talpid3 and Cep290 play overlapping and distinct roles in cilia assembly. *J. Cell Biol.* **204**, 215-229. doi:10.1083/jcb.201304153

Kodani, A., Yu, T. W., Johnson, J. R., Jayaraman, D., Johnson, T. L., Al-Gazali, L., Sztriha, L., Partlow, J. N., Kim, H., Krup, A. L. et al. (2015). Centriolar satellites assemble centrosomal microcephaly proteins to recruit CDK2 and promote centriole duplication. *eLife* **4**, e07519. doi:10.7554/eLife.07519

Kubo, A. and Tsukita, S. (2003). Non-membranous granular organelle consisting of PCM-1: subcellular distribution and cell-cycle-dependent assembly/disassembly. *J. Cell Sci.* **116**, 919-928. doi:10.1242/jcs.00282

Li, S., Sandercock, A. M., Conduit, P., Robinson, C. V., Williams, R. L. and Kilmartin, J. V. (2006). Structural role of Sfi1p-centrin filaments in budding yeast spindle pole body duplication. *J. Cell Biol.* **173**, 867-877. doi:10.1083/jcb.200603153

Li, J., D'angiolella, V., Seeley, E. S., Kim, S., Kobayashi, T., Fu, W., Campos, E. I., Pagano, M. and Dynlacht, B. D. (2013). USP33 regulates centrosome biogenesis via deubiquitination of the centriolar protein CP110. *Nature* **495**, 255-259. doi:10.1038/nature11941

Löffler, H., Fechter, A., Liu, F. Y., Poppelreuther, S. and Krämer, A. (2013). DNA damage-induced centrosome amplification occurs via excessive formation of centriolar satellites. *Oncogene* **32**, 2963-2972. doi:10.1038/onc.2012.310

Martinez-Sanz, J., Yang, A., Blouquit, Y., Duchambon, P., Assairi, L. and Craescu, C. T. (2006). Binding of human centrin 2 to the centrosomal protein hSfi1. *FEBS J.* **273**, 4504-4515. doi:10.1111/j.1742-4658.2006.05456.x

Matei, E., Miron, S., Blouquit, Y., Duchambon, P., Durussel, I., Cox, J. A. and Craescu, C. T. (2003). C-terminal half of human centrin 2 behaves like a regulatory EF-hand domain. *Biochemistry* **42**, 1439-1450. doi:10.1021/bi0269714

Middendorp, S., Küntziger, T., Abraham, Y., Holmes, S., Bordes, N., Paintrand, M., Paoletti, A. and Bornens, M. (2000). A role for centrin 3 in centrosome reproduction. *J. Cell Biol.* **148**, 405-416. doi:10.1083/jcb.148.3.405

Mikule, K., Delaval, B., Kaldis, P., Jurcyzk, A., Hergert, P. and Doxsey, S. (2007). Loss of centrosome integrity induces p38-p53-p21-dependent G1-S arrest. *Nat. Cell Biol.* **9**, 160-170. doi:10.1038/ncb1529

Nishi, R., Okuda, Y., Watanabe, E., Mori, T., Iwai, S., Masutani, C., Sugasawa, K. and Hanaoka, F. (2005). Centrin 2 stimulates nucleotide excision repair by interacting with xeroderma pigmentosum group C protein. *Mol. Cell. Biol.* **25**, 5664-5674. doi:10.1128/MCB.25.13.5664-5674.2005

Nishi, R., Sakai, W., Tone, D., Hanaoka, F. and Sugasawa, K. (2013). Structure-function analysis of the EF-hand protein centrin-2 for its intracellular localization and nucleotide excision repair. *Nucleic Acids Res.* **41**, 6917-6929. doi:10.1093/nar/gkt434

Oda, T., Chiba, S., Nagai, T. and Mizuno, K. (2014). Binding to Cep164, but not EB1, is essential for centriolar localization of TTBK2 and its function in ciliogenesis. *Genes Cells* **19**, 927-940. doi:10.1111/gtc.12191

Odabasi, E., Gul, S., Kavakli, I. H. and Firat-Karalar, E. N. (2019). Centriolar satellites are required for efficient ciliogenesis and ciliary content regulation. *EMBO Rep.* **20**, e47723. doi:10.15252/embr.201947723

Ogungbenro, Y. A., Tena, T. C., Gaboriau, D., Lalor, P., Dockery, P., Philipp, M. and Morrison, C. G. (2018). Centrobin controls primary ciliogenesis in vertebrates. *J. Cell Biol.* **217**, 1205-1215. doi:10.1083/jcb.201706095

Ohta, T., Essner, R., Ryu, J.-H., Palazzo, R. E., Uetake, Y. and Kuriyama, R. (2002). Characterization of Cep135, a novel coiled-coil centrosomal protein involved in microtubule organization in mammalian cells. *J. Cell Biol.* **156**, 87-99. doi:10.1083/jcb.200108088

Ortiz, M., Sanoguet, Z., Hu, H., Chazin, W. J., McMurray, C. T., Salisbury, J. L. and Pastrana-Rios, B. (2005). Dynamics of hydrogen-deuterium exchange in Chlamydomonas centrin. *Biochemistry* **44**, 2409-2418. doi:10.1021/bi0484419

Paoletti, A., Moudjou, M., Paintrand, M., Salisbury, J. L. and Bornens, M. (1996). Most of centrin in animal cells is not centrosome-associated and centrosomal centrin is confined to the distal lumen of centrioles. *J. Cell Sci.* **109**, 3089-3102.

Prosser, S. L. and Morrison, C. G. (2015). Centrin 2 regulates CP110 removal in primary cilium formation. *J. Cell Biol.* **208**, 693-701. doi:10.1083/jcb.201411070

Prosser, S. L., Straatman, K. R. and Fry, A. M. (2009). Molecular dissection of the centrosome overduplication pathway in S-phase-arrested cells. *Mol. Cell. Biol.* **29**, 1760-1773. doi:10.1128/MCB.01124-08

Quarantotti, V., Chen, J. X., Tischer, J., Gonzalez Tejedo, C., Papachristou, E. K., D'santos, C. S., Kilmartin, J. V., Miller, M. L. and Gergely, F. (2019). Centriolar satellites are acentriolar assemblies of centrosomal proteins. *EMBO J.* **38**, e101082. doi:10.15252/embj.2018101082

Radu, L., Durussel, I., Assairi, L., Blouquit, Y., Miron, S., Cox, J. A. and Craescu, C. T. (2010). Scherffelia dubia centrin exhibits a specific mechanism for Ca(2+)-controlled target binding. *Biochemistry* **49**, 4383-4394. doi:10.1021/bi901764m

Rust, M. J., Bates, M. and Zhuang, X. (2006). Sub-diffraction-limit imaging by stochastic optical reconstruction microscopy (STORM). *Nat. Methods* **3**, 793-795. doi:10.1038/nmeth929

Salisbury, J. L., Suino, K. M., Busby, R. and Springett, M. (2002). Centrin-2 is required for centriole duplication in mammalian cells. *Curr. Biol.* **12**, 1287-1292. doi:10.1016/S0960-9822(02)01019-9

Sánchez, I. and Dynlacht, B. D. (2016). Cilium assembly and disassembly. *Nat. Cell Biol.* **18**, 711-717. doi:10.1038/ncb3370

Schmidt, T. I., Kleylein-Sohn, J., Westendorf, J., Le Clech, M., Lavoie, S. B., Stierhof, Y. D. and Nigg, E. A. (2009). Control of centriole length by CPAP and CP110. *Curr. Biol.* **19**, 1005-1011. doi:10.1016/j.cub.2009.05.016

Sorokin, S. (1962). Centrioles and the formation of rudimentary cilia by fibroblasts and smooth muscle cells. *J. Cell Biol.* **15**, 363-377. doi:10.1083/jcb.15.2.363

Spang, A., Courtney, I., Grein, K., Matzner, M. and Schiebel, E. (1995). The Cdc31p-binding protein Kar1p is a component of the half bridge of the yeast spindle pole body. *J. Cell Biol.* **128**, 863-877. doi:10.1083/jcb.128.5.863

Spektor, A., Tsang, W. Y., Khoo, D. and Dynlacht, B. D. (2007). Cep97 and CP110 suppress a cilia assembly program. *Cell* **130**, 678-690. doi:10.1016/j.cell.2007.06.027

Stemm-Wolf, A. J., Morgan, G., Giddings, T. H., Jr, White, E. A., Marchione, R., Mcdonald, H. B. and Winey, M. (2005). Basal body duplication and maintenance require one member of the Tetrahymena thermophila centrin gene family. *Mol. Biol. Cell* **16**, 3606-3619. doi:10.1091/mbc.e04-10-0919

Tang, C.-J. C., Fu, R.-H., Wu, K. S., Hsu, W.-B. and Tang, T. K. (2009). CPAP is a cell-cycle regulated protein that controls centriole length. *Nat. Cell Biol.* **11**, 825-831. doi:10.1038/ncb1889

Tanos, B. E., Yang, H.-J., Soni, R., Wang, W.-J., Macaluso, F. P., Asara, J. M. and Tsou, M.-F. B. (2013). Centriole distal appendages promote membrane docking, leading to cilia initiation. *Genes Dev.* **27**, 163-168. doi:10.1101/gad.207043.112

Tollenaere, M. A. X., Mailand, N. and Bekker-Jensen, S. (2015). Centriolar satellites: key mediators of centrosome functions. *Cell. Mol. Life Sci.* **72**, 11-23. doi:10.1007/s00018-014-1711-3

Tourbez, M., Firanescu, C., Yang, A., Unipan, L., Duchambon, P., Blouquit, Y. and Craescu, C. T. (2004). Calcium-dependent self-assembly of human centrin 2. *J. Biol. Chem.* **279**, 47672-47680. doi:10.1074/jbc.M404996200

Tsang, W. Y. and Dynlacht, B. D. (2013). CP110 and its network of partners coordinately regulate cilia assembly. *Cilia* **2**, 9. doi:10.1186/2046-2530-2-9

Tsang, W. Y., Spektor, A., Luciano, D. J., Indjeian, V. B., Chen, Z., Salisbury, J. L., Sanchez, I. and Dynlacht, B. D. (2006). CP110 cooperates with two calcium-binding proteins to regulate cytokinesis and genome stability. *Mol. Biol. Cell* **17**, 3423-3434. doi:10.1091/mbc.e06-04-0371

Tsang, W. Y., Bossard, C., Khanna, H., Peranen, J., Swaroop, A., Malhotra, V. and Dynlacht, B. D. (2008). CP110 suppresses primary cilia formation through its interaction with CEP290, a protein deficient in human ciliary disease. *Dev. Cell* **15**, 187-197. doi:10.1016/j.devcel.2008.07.004

Veeraraghavan, S., Fagan, P. A., Hu, H., Lee, V., Harper, J. F., Huang, B. and Chazin, W. J. (2002). Structural independence of the two EF-hand domains of caltractin. *J. Biol. Chem.* **277**, 28564-28571. doi:10.1074/jbc.M112232200

Vonderfecht, T., Stemm-Wolf, A. J., Hendershott, M., Giddings, T. H., Jr, Meehl, J. B. and Winey, M. (2011). The two domains of centrin have distinct basal body functions in Tetrahymena. *Mol. Biol. Cell* **22**, 2221-2234. doi:10.1091/mbc.e11-02-0151

Wang, W., Zhao, Y., Wang, H. and Yang, B. (2018). Crystal structure of the trimeric N-terminal domain of ciliate Euplotes octocarinatus centrin binding with calcium ions. *Protein Sci.* **27**, 1102-1108. doi:10.1002/pro.3418

Wiech, H., Geier, B. M., Paschke, T., Spang, A., Grein, K., Steinkotter, J., Melkonian, M. and Schiebel, E. (1996). Characterization of green alga, yeast, and human centrins. Specific subdomain features determine functional diversity. *J. Biol. Chem.* **271**, 22453-22461. doi:10.1074/jbc.271.37.22453

Yadav, S. P., Sharma, N. K., Liu, C., Dong, L., Li, T. and Swaroop, A. (2016). Centrosomal protein CP110 controls maturation of the mother centriole during cilia biogenesis. *Development* **143**, 1491-1501. doi:10.1242/dev.130120

Yang, A., Miron, S., Duchambon, P., Assairi, L., Blouquit, Y. and Craescu, C. T. (2006). The N-terminal domain of human centrin 2 has a closed structure, binds calcium with a very low affinity, and plays a role in the protein self-assembly. *Biochemistry* **45**, 880-889. doi:10.1021/bi051397s

Yang, T. T., Chong, W. M., Wang, W. J., Mazo, G., Tanos, B., Chen, Z., Tran, T. M. N., Chen, Y. D., Weng, R. R., Huang, C. E. et al. (2018). Super-resolution architecture of mammalian centriole distal appendages reveals distinct blade and matrix functional components. *Nat. Commun.* **9**, 2023. doi:10.1038/s41467-018-04469-1

Ying, G., Avasthi, P., Irwin, M., Gerstner, C. D., Frederick, J. M., Lucero, M. T. and Baehr, W. (2014). Centrin 2 is required for mouse olfactory ciliary trafficking and development of ependymal cilia planar polarity. *J. Neurosci.* **34**, 6377-6388. doi:10.1523/JNEUROSCI.0067-14.2014

Zhang, Y. and He, C. Y. (2011). Centrins in unicellular organisms: functional diversity and specialization. *Protoplasma* **249**, 459-467. doi:10.1007/s00709-011-0305-2